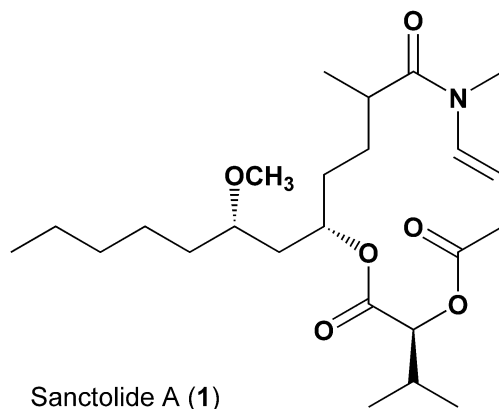


## Graphical Abstract

**Sanctolide A, a 14-membered PK-NRP hybrid macrolide from the cultured cyanobacterium *Oscillatoria sancta* (SAG 74.79)**

Hahk-Soo Kang, Aleksej Kronic, Jimmy Orjala

Leave this area blank for abstract info.



Address for correspondence:

Jimmy Orjala, Department of Medicinal Chemistry and Pharmacognosy, College of Pharmacy, 833

South Wood Street, University of Illinois at Chicago, Chicago, IL 60612, USA

(M/C781)

Tel: 312-996-5583

Fax: 312-996-7107

E-mail: [orjala@uic.edu](mailto:orjala@uic.edu)

# Sanctolide A, a 14-membered PK-NRP hybrid macrolide from the cultured cyanobacterium *Oscillatoria sancta* (SAG 74.79)

Hahk-Soo Kang, Aleksej Krunic, and Jimmy Orjala\*

Department of Medicinal Chemistry and Pharmacognosy, College of Pharmacy, University of Illinois at Chicago, Chicago, IL 60612, USA

**Abstract:** Sanctolide A (**1**), a 14-membered polyketide-nonribosomal peptide (PK-NRP) hybrid macrolide, was isolated from the cultured cyanobacterium *Oscillatoria sancta* (SAG 74.79). The planar structure was determined using various spectroscopic techniques including HRESIMS, and 1D and 2D NMR analyses. The relative configuration was assigned by *J*-based configurational analysis in combination with NOE correlations. The absolute configuration was determined by Mosher ester and enantioselective HPLC analyses. The structure of sanctolide A (**1**) features a rare *N*-methyl enamide and a 2-hydroxyisovaleric acid, which are incorporated to form a 14-membered macrolide ring structure, comprising a new type of cyanobacterial macrolides derived from a PKS-NRPS hybrid biosynthetic pathway.

**Keywords:** cyanobacteria, *Oscillatoria sancta*, 14-membered macrolide, PK-NRP hybrid, brine shrimp toxicity

Cyanobacteria (blue-green algae) have been shown to be prolific producers of bioactive secondary metabolites.<sup>1-3</sup> Polyketide-nonribosomal peptide (PK-NRP) hybrids represent a major class of cyanobacterial secondary metabolites.<sup>4</sup> Diverse cyanobacterial metabolites belonging to this class have been isolated from both freshwater and marine cyanobacteria. A major group of cyanobacterial PK-NRP hybrid metabolites is lipopeptides, where linear or cyclic peptides contain one lipophilic residue of polyketide origin such as  $\beta$ -amino acid and *N*-acyl residues.<sup>2</sup> Another subclass of cyanobacterial PK-NRP hybrid metabolites is comprised of macrolides whose building blocks are mainly acetates with one or two amino acids incorporated into their macrolide ring structures. These compounds are less commonly found in cyanobacteria. Examples include laingolide, laingolides A and B, madangolide and palmyrolide A, all of which have 15-membered macrolide rings containing a rare *N*-methyl enamide functionality.<sup>5-8</sup> These metabolites were all obtained from marine cyanobacteria belonging to the order Oscillatoriales.

In our continuing search for biologically active secondary metabolites from cultured cyanobacteria, the cell extract of *Oscillatoria sancta* (SAG 74.79) was initially evaluated for its activity in a brine shrimp toxicity assay and found to be active. Herein, we report the isolation and structure determination of a 14-membered PK-NRP hybrid macrolide, named sanctolide A (**1**). The planar structure was determined using spectroscopic techniques including HRESIMS, and 1D and 2D NMR analyses. The relative configuration of **1** was solved by *J*-based configurational analysis along with NOE correlations, and Mosher ester and enantioselective HPLC analyses were carried out for the assignment of the absolute configuration.

*Oscillatoria sancta* was obtained from the SAG (Sammlung von Algenkulturen Göttingen) culture collection of algae (strain ID: 74.79), and grown in inorganic media (BG-12).<sup>9</sup> The freeze-dried cells were extracted with a mixture of CH<sub>2</sub>Cl<sub>2</sub>-MeOH (1:1 v/v). This organic extract was fractionated

using Diaion HP-20 resin with an increasing amount of iPrOH in water. The fractions eluting at 70% and 80% iPrOH displayed toxicity against brine shrimp. HPLC-based activity profiling of these fractions using reversed-phase column identified one minor peak as the active component (Figure S2 in Supplementary data). Dereplication by LC-MS and  $^1\text{H}$  NMR indicated this peak to be a potentially new metabolite with a molecular weight of 439 Da. Scale-up culture ( $4 \times 2\text{L}$ ) and re-isolation was performed using the method described above followed by reversed-phase HPLC to yield sanctolide A (**1**, 2.6 mg, Figure 1).

Sanctolide A (**1**)<sup>10</sup> was obtained as colorless oil. The molecular formula of **1** was established as  $\text{C}_{24}\text{H}_{41}\text{NO}_6$  by HRESIMS analysis. Analysis of the  $^1\text{H}$  NMR spectrum of **1** in combination with the DEPT-Q and HSQC spectra indicated the presence of two olefinic protons ( $\delta_{\text{H}}$  6.70 and 5.12), three oxygenated methines ( $\delta_{\text{H}}$  5.11, 5.00 and 3.12), one *O*-methyl ( $\delta_{\text{H}}$  3.28), one *N*-methyl ( $\delta_{\text{H}}$  3.06), two methines ( $\delta_{\text{H}}$  2.56 and 2.31), five diastereotopic methylenes ( $\delta_{\text{H}}$  2.0 – 1.0), three homotopic methylenes ( $\delta_{\text{H}}$  1.28 and 1.24), as well as three doublet ( $\delta_{\text{H}}$  1.13, 0.94 and 0.90) and one triplet methyl ( $\delta_{\text{H}}$  0.87) protons. Analysis of the COSY spectrum established three partial structures **1a**, **1b** and **1c** (Figure 2). The first partial structure (**1a**) was assembled by sequential COSY correlations from H-2 ( $\delta_{\text{H}}$  2.56) to H<sub>3</sub>-12 ( $\delta_{\text{H}}$  0.87) along with a COSY correlation between H-2 and H<sub>3</sub>-13 methyl ( $\delta_{\text{H}}$  1.13). Down-field chemical shifts of H-5 ( $\delta_{\text{H}}$  5.00) and H-7 ( $\delta_{\text{H}}$  3.12) indicated that C-5 and C-7 were oxygenated. The second partial structure (**1b**) was established from COSY correlations between H-15 ( $\delta_{\text{H}}$  5.11) and H-16 ( $\delta_{\text{H}}$  2.31), and between H-16 and H<sub>3</sub>-17/H<sub>3</sub>-18 methyl protons ( $\delta_{\text{H}}$  0.94/0.90). A downfield chemical shift of H-15 ( $\delta_{\text{H}}$  5.11) and the absence of a NH signal indicated this partial structure to be a 2-hydroxyisovaleric acid. This was further supported by chemical shifts of C-15 ( $\delta_{\text{C}}$  77.0) and C-19 ( $\delta_{\text{C}}$  168.7). COSY correlations between H-20 ( $\delta_{\text{H}}$  3.20 and 3.15)/H-21 ( $\delta_{\text{H}}$  5.12)/H-22 ( $\delta_{\text{H}}$  6.70) determined

the last partial structure as a 1, 3-functionalized propylene (**1c**) possessing the *trans* geometry due to the large  $^3J_{\text{HH}}$  (14.0 Hz) observed between H-21 and H-22.

The three partial structures (**1a**, **1b** and **1c**) were assembled through HMBC correlations (Figure 2). An HMBC correlation from the *O*-methyl singlet ( $\delta_{\text{H}}$  3.28) to C-7 methine ( $\delta_{\text{C}}$  77.7) placed a methoxy group at C-7. The chemical shift of C-14 ( $\delta_{\text{C}}$  170.0) combined with HMBC correlations from H-5 ( $\delta_{\text{H}}$  5.00) and H-16 ( $\delta_{\text{H}}$  2.31) to C-14 allowed the assembly of partial structures **1a** and **1b** via an ester linkage. The connection between substructures **1b** and **1c** was established by HMBC correlations from H-15 ( $\delta_{\text{H}}$  5.11) and H-21 ( $\delta_{\text{H}}$  5.12) to C-19 ( $\delta_{\text{C}}$  168.7), positioning the 2-hydroxyisovaleric acid between **1a** and **1c** via two ester linkages. HMBC correlations from an *N*-methyl singlet ( $\delta_{\text{H}}$  3.06) to C-22 ( $\delta_{\text{C}}$  132.4) and C-1 ( $\delta_{\text{C}}$  174.5), and from H<sub>3</sub>-13 ( $\delta_{\text{H}}$  1.13) to C-1 linked **1a** and **1c** through the *N*-methyl enamide bridge, completing the assembly of a 14-membered macrolide ring scaffold.

The relative configuration between C5 and C7 was determined by *J*-based configurational analysis<sup>11</sup> in combination with NOE correlations (Figure 3). Homonuclear ( $^3J_{\text{HH}}$ ) and heteronuclear ( $^2J_{\text{CH}}$  and  $^3J_{\text{CH}}$ ) coupling constants were obtained from the DQF-COSY and GBIRD-HSQMBC spectra, respectively.<sup>12, 13</sup> A small  $^3J_{\text{H5H6a}}$  (3.8 Hz) and a large  $^3J_{\text{H5H6b}}$  (8.1 Hz) indicated the *gauche* conformation between H-5 and H-6a and the *anti* conformation between H-5 and H-6b, respectively, leaving A3 and A4 as two possible conformations (Figure S3 in Supplementary data). An NOE correlation observed between H<sub>2</sub>-4 and H-6a indicated A4 to be the only possible conformation, allowing the stereospecific assignments of the diastereotopic protons H-6a/b (Figure 3). For the C6-C7 bond, only two conformations B1 and B5 were possible based on a large  $^3J_{\text{H6aH7}}$  (9.0 Hz) and a small  $^3J_{\text{H6bH7}}$  (2.9 Hz) (Figure S3 in Supplementary data). An NOE correlation observed between H-6b and H<sub>2</sub>-8 and between H-5 and OMe left B1 as the only possible conformation, thus allowing the assignment of the *anti* configuration for the 1,3-methine system at C5-C7. Determination of the relative

configuration for the 1,4-methine system between C-2 and C-5 using NMR methods was complicated as analysis of the NOE spectrum indicated the presence of multiple conformations for the macrolide ring in **1**. The proton H-5 showed NOE correlations with all of four diastereotopic protons including H-3a/b and H-4a/b, and a NOESY experiment recorded with a short mixing time (200 ms) verified these cross-peaks to be real NOE correlations as opposed to artifacts arising from spin diffusion. A *J*-based configurational analysis was attempted but unsuccessful due to a number of medium *J* values observed for this 1,4 methine system. Attempts to crystallize **1** were also unsuccessful due to the labile nature of an enamide moiety and the presence of a 12 carbons-long fatty acid branch. Therefore, the configuration of a stereocenter at C-2 could not be assigned.

The absolute configuration at C-5, C-7 and C-15 was established by Mosher ester and enantioselective HPLC analyses (Figure 4). <sup>1</sup>H NMR and LC-MS analyses indicated that acid hydrolysis of **1** resulted in the formation of **2** due to the labile nature of an enamide moiety under acidic conditions, similar as reported for palmyrolide A by Pereira et al.<sup>7</sup> The isolation of **2** from the acid hydrolysate was necessary for Mosher ester analysis, but challenging due to the lack of a chromophore. Alternatively, solvolysis of **1** was carried out using NaOMe in MeOH, and the resulting product was dried *in vacuo* for 24 hrs. <sup>1</sup>H NMR and LC-MS analyses identified the presence of **2** as a sole product<sup>14</sup> probably due to volatile nature of the other methyl ester products. The resulting solvolysis product was subjected to Mosher ester analysis. Two equal portions of **2** were derivatized with (*R*)- and (*S*)-MTPA chlorides at C-5 to yield (*S*)- and (*R*)-MTPA esters (**2S** and **2R**), respectively.<sup>15, 16</sup> Interpretation of the <sup>1</sup>H NMR chemical shift differences ( $\Delta\delta_{S-R}$ ) between **2S** and **2R** assigned the *S* configuration to C-5, thereby leading to the assignment of the absolute configuration as *5S,7S*. The absolute configuration of the remaining 2-hydroxyisovaleric acid residue (**3**) was assigned by enantioselective HPLC analysis of the acid hydrolysate.<sup>17</sup> Comparison of the retention times between the acid hydrolysate of **1** and two

authentic standards *L*- and *D*-2-hydroxyisovaleric acids allowed the absolute configuration of **3** to be assigned as *L*.

As observed for other enamide-containing natural products,<sup>5-8</sup> compound **1** was highly labile and underwent rapid enamide hydrolysis in the presence of water or acid, resulting in an opening of the macrolide ring. Pereira et al. proposed the mechanism of enamide hydrolysis in acidic conditions.<sup>7</sup> This enamide hydrolysis can also occur in neutral pH in a similar manner and involves the reversible conversion of the enamide moiety into an iminium ion, which undergoes addition by water followed by proton transfer, leading to the formation of a secondary amide and an aldehyde (Figure 5). A degradation experiment indicated that the enamide of **1** was completely hydrolyzed in 48 hrs at rt upon addition of water at similar concentrations used in our biological assay systems, indicating that the macrolide ring structure would be degraded during biological evaluation (see Supplementary data). Sanctolide A (**1**) exhibited moderate toxicity to brine shrimp with an LD<sub>50</sub> value of 23.5 μM. Compound **1** was also evaluated for its cytotoxicity against the HT-29 and MDA-MB-435 cell lines as well as antibacterial activity against *E. coli* and *S. aureus*, but no activity was found in either assay system at the highest concentration tested (25 μg/mL). Based on the degradation observed above, it is suggested that compound **1** was present in the acyclic form during the biological evaluation, and this acyclic form of **1** was moderately toxic to brine shrimp.

Sanctolide A (**1**) features a new class of cyanobacterial macrolides where two amino acid precursors Gly and Val are incorporated into a polyketide chain to form a 14-membered macrolide ring structure. The biosynthesis of **1** was proposed as follows: The first step of biosynthesis involves the formation of a hexaketide (C1 – C12) chain by six PKS modules with  $\alpha$ -branched methyl (C-13), which is likely originated from *S*-adenosyl-*L*-methionine (SAM).<sup>18</sup> This hexaketide chain is further expanded with *N*-methyl glycine by a NRPS module followed by ketide extension by one acetate unit, reduction,

dehydration and double bond isomerization, resulting in the formation of the C21-C22 enamide functionality as proposed for the palmyrolide A.<sup>7</sup> The 2-hydroxyisovaleric acid linked to the hydroxyl group at C-5 is likely formed by transamination of Val followed by reduction.<sup>18</sup> The cyclization between C-15 hydroxyl and C-19 carboxyl group is likely to occur in a final step, thus completing the proposed biosynthesis of **1**.

**Acknowledgments:** This research was supported by PO1 CA125066 from NCI/NIH. We thank Dr. B. Ramirez from Center for Structural Biology at UIC for providing an access to 600 and 900 MHz NMR spectrometers. We also thank Q. Shen and Dr. S. M. Swanson for performing cytotoxicity assays, and Drs. S. Cho and S. Franzblau from the Institute for Tuberculosis Research (ITR) at UIC for conducting anti-fungal and anti-bacterial assays. LC-MS and HRESIMS analyses were performed at UIC Research Resource Center (RRC) Mass Spectrometry Facility.

**Supplementary Data:** Experimental detail; HPLC-based activity profiling; the full list of rotamers for *J*-based configurational analysis; <sup>1</sup>H NMR, COSY, HSQC, HMBC, DQF-COSY, HSQMBC and NOESY spectra of **1**; <sup>1</sup>H NMR spectra of **2**, **2S** and **2R**; <sup>1</sup>H NMR spectra of the degraded products.

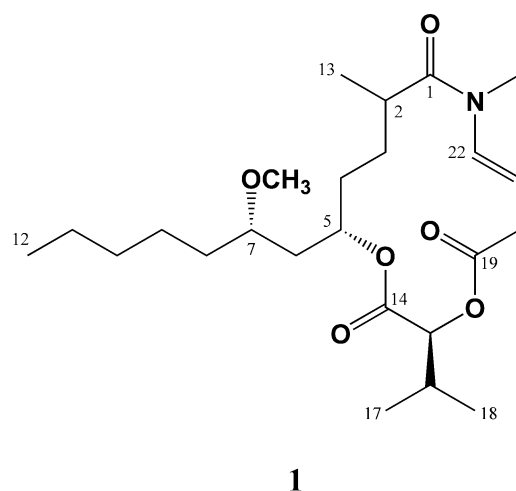


**Figure 1.** The structure of sanctolide A (**1**).

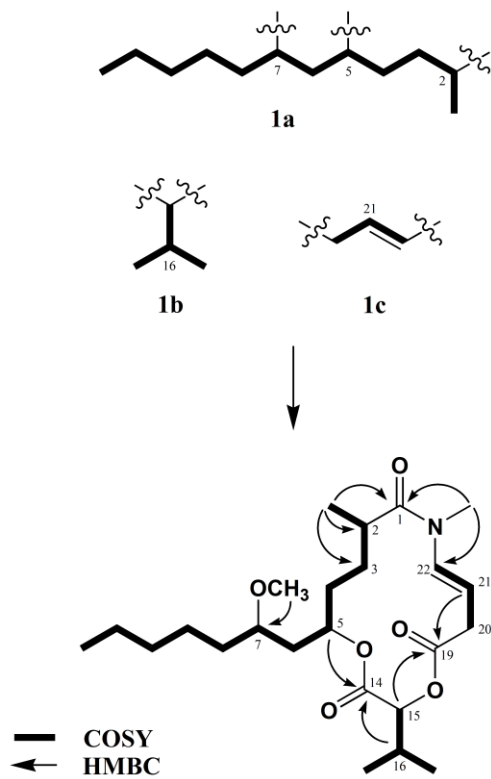


**Figure 2.** Key 2D NMR correlations used to determine the planar structure of **1**.

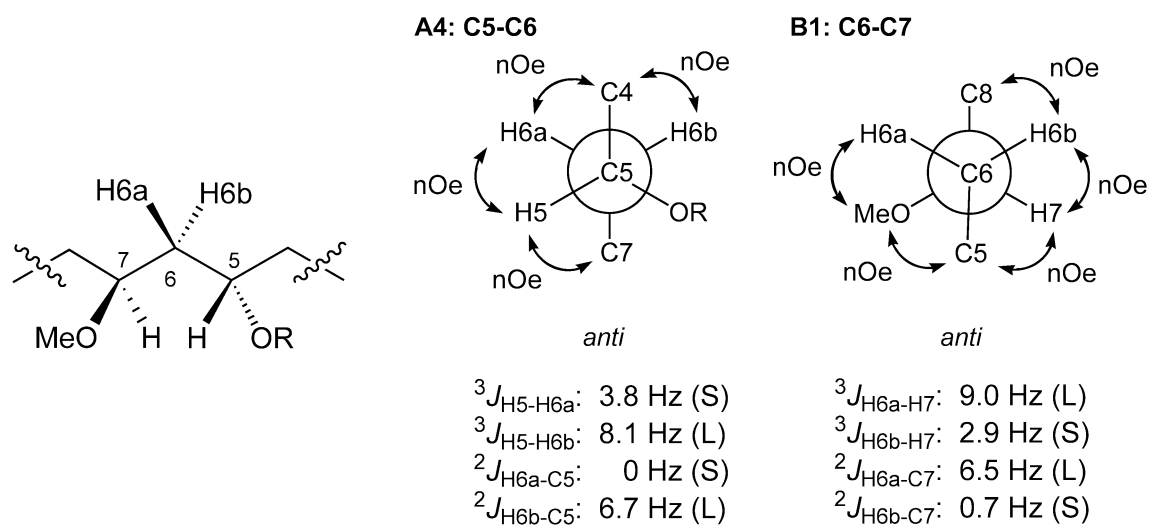


**Figure 3.** Newman projections for A4: C5-C6 and B1: C6-C7. The DQF-COSY and GBIRD-HSQMBC spectra were used for the measurement of homo- and hetero-nuclear coupling constants. Labels in parentheses denote the predicted size of coupling constants: S-small, M-medium and L-large. No correlation observed in the HSQMBC spectrum was assigned as a coupling of 0 Hz. Observed nOe correlations are presented as arched arrows. A full list of rotamers can be found in Supplementary data.

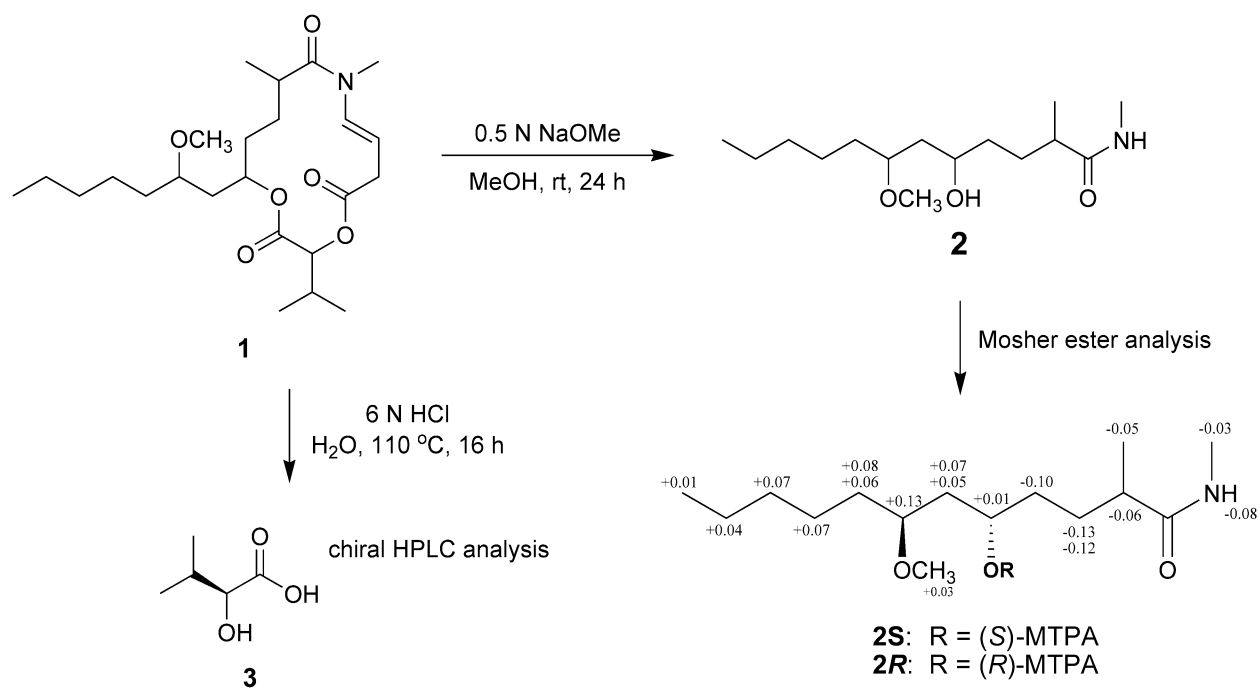


**Figure 4.** Methanolysis and acid hydrolysis for the absolute configuration of **1** at C-5 and C-15;  $\Delta\delta_{S-R}$

values ( $\Delta\delta_{S-R} = \delta_S - \delta_R$ ) for the MTPA esters **2S** and **2R**.

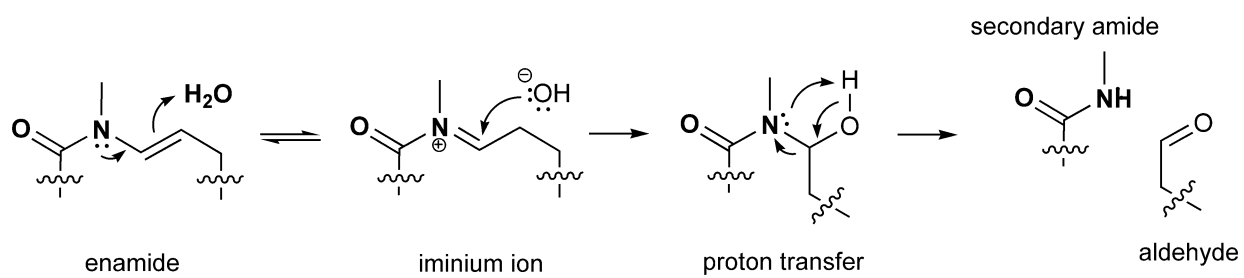


**Figure 5.** Proposed enamide hydrolysis of **1** in neutral pH that leads to ring-opening of the macrolide ring structure.

**Table 1**  
NMR spectroscopic data for sanctolide A (**1**) in CDCl<sub>3</sub>

	sanctolide A ( <b>1</b> )					
	$\delta_C^{a,c}$	$\delta_H^{b,c}$	mult.( <i>J</i> in Hz)	COSY <sup>b</sup>	HMBC <sup>b</sup>	NOESY <sup>b,d</sup>
1	174.5					
2	38.1	2.56	m	3, 13	1, 3, 4, 13	3b, 4a, 13, 22
3 <sup>a</sup>	29.2	1.21	m	2, 4	1, 2, 4, 5, 13	3b, 4b, 13
3 <sup>b</sup>		1.68	m			2, 3a, 4a, 5
4 <sup>a</sup>	34.1	1.42	m	3, 5	2, 3	3b, 4b, 13
4 <sup>b</sup>		1.86	m			3a, 4a, 5, 13
5	73.3	5.00	m	4, 6	3, 4, 6, 7, 14	3a, 3b, 4a, 4b, 6a, 6b, 7, OMe
6 <sup>a</sup>	40.3	1.59	ddd (14.4, 9.0, 4.2)	5, 7	4, 5, 7, 8	4a, 4b, 6b, 7, OMe
6 <sup>b</sup>		1.74	ddd (14.4, 7.8, 3.0)			6a, 5, 7, 8a, 8b
7	77.7	3.12	m	6, 8	5, 6, O-Me	5, 6a, 6b, 7, 8a, 8b
8 <sup>a</sup>	33.2	1.37	m	7, 9	6, 7, 9, 10	6a, 6b, 8b
8 <sup>b</sup>		1.50	m			6b, 7, 8a, OMe
9	32.0	1.24	m	8, 10	7, 8, 10, 11	
10	24.3	1.24	m	9, 11	8, 9, 11, 12	
11	22.6	1.28	m	10, 12	9, 10, 12	
12	14.2	0.87	t (7.1)	11	10, 11	
13	14.9	1.13	d (6.9)	2	1, 2, 3	2, 3a, 4a, 4b
14	170.0					
15	77.0	5.11	d (6.4)	16	14, 16, 17, 18, 19	16, 17, 18
16	29.6	2.31	sd (6.8, 6.4)	15, 17, 18	14, 15, 17, 18	15, 17, 18
17	18.6	0.94	d (6.8)	16, 18	15, 16, 18	
18	17.2	0.90	d (6.8)	16, 17	15, 16, 17	
19	168.7					
20	34.5	3.15	dd (6.5, 1.3)	21	19, 21, 22	21, 22
		3.20	d (6.9)			
21	102.7	5.12	m	20	19, 20, 22	20, 22, NMe
22	132.4	6.70	d (14.0)	21	1, 20, N-Me	2, 3b, 20, 21, NMe
O-Me	56.6	3.28	s		7	5, 6a, 8a, 8b, 17
N-Me	30.6	3.06	s		1, 22	21, 22

<sup>a</sup> assigned using the DEPT-Q spectrum recorded at 226 MHz, <sup>b</sup> recorded at 600 MHz, <sup>c</sup> chemical shifts were referenced to the CDCl<sub>3</sub> solvent signals ( $\delta_H$  7.24 and  $\delta_C$  77.2). <sup>d</sup> mixing time: 600 ms

## References and notes:

1. Tan, L. T. *Phytochemistry* **2007**, 68, 954-979.
2. Wagoner, R. M. V.; Drummond, A. K.; Wright, J. L. C. *Adv. Appl. Microbiol* **2007**, 89-217.
3. Chlipala, G. E.; Mo, S.; Orjala, J. *Curr. Drug Targets* **2011**, 12, 1654-1673.
4. Singh, S.; Kate, B. N.; Banerjee, U. C. *Critical. Rev. Biotech* **2005**, 25, 73-95.
5. Klein, D.; Braekman, J. C.; Daloz, D. *Tetrahedron Lett.* **1996**, 37, 7519-7520.
6. Klein, D.; Braekman, J. C.; Daloz, D.; Hoffmann, L.; Castillo, G.; Demoulin, V. *J. Nat. Prod.* **1999**, 62, 934-936.
7. Pereira, A. R.; Cao, Z.; Engene, N.; Soria-Mercado, I. E.; Murray, T. F.; Gerwick, W. H. *Org. Lett.*, **2010**, 12, 4490-4493.
8. Matthew, S.; Salvador, L. A.; Schupp, P. J.; Paul, V. J.; Luesch, H. *J. Nat. Prod.* **2010**, 73, 1544-1552.
9. Falch, B. S.; Konig, G. M.; Wright, A. D.; Sticher, O.; Angerhofer, C. K.; Pezzuto, J. M.; Bachmann, H. *Planta Med.* **1995**, 61, 321-328.
10. Sanctolide A (**1**): colorless oil;  $[\alpha]_D^{25}$  - 41 (*c* 0.1, MeOH); UV (MeOH)  $\lambda_{\max}$  (log  $\epsilon$ ) 234 (3.77) nm; IR (neat)  $\nu_{\max}$  2964, 2928, 1736, 1678, 1638  $\text{cm}^{-1}$ ; 1D and 2D NMR data, see Table 1; HRESIMS  $m/z$  440.3005  $[\text{M}+\text{H}]^+$  (calcd for  $\text{C}_{24}\text{H}_{42}\text{NO}_6$ , 440.3012)
11. Matsumori, N.; Kaneno, D.; Murata, M.; Nakamura, H.; Tachibana, K. *J. Org. Chem.* 1999, 64, 866-876.

12. Rance, M.; Sørensen, O. W.; Bodenhausen, G.; Wagner, G.; Ernst, R. R.; Wüthrich, K. *Biochem. Biophys. Res. Commun.* **1983**, 117, 479-485.
13. Williamson, R. T.; Márquez, B. L.; Gerwick, W. H.; Kövér, K. E. *Magn. Reson. Chem.* **2000**, 38, 265-273.
14. Methanolysis of **1**: A portion of **1** (1.2 mg) was treated with 1 mL of 0.5 N NaOMe in MeOH and stirred for 24 h at 25°C. The resulting mixture was extracted with CH<sub>2</sub>Cl<sub>2</sub> two times and dried *in vacuo* overnight to give 0.8 mg of **2** as a sole product. Compound **2**: colorless oil; <sup>1</sup>H NMR data (600 MHz, CDCl<sub>3</sub>) δ 5.58 (1H, m, NH), 3.87 (1H, m, H-5), 3.44 (1H, m, H-7), 3.34 (3H, s, OCH<sub>3</sub>), 2.78 (3H, d, *J* = 4.6 Hz, NCH<sub>3</sub>), 2.23 (1H, m, H-2), 1.73 (1H, m, H-3b), 1.67 (1H, ddd, *J* = 14.6, 8.9 and 2.9 Hz, H-6b), 1.60 (1H, m, H-8a), 1.52 (1H, ddd, *J* = 14.6, 6.4 and 1.4 Hz, H-6a), 1.44 (1H, m, H-3a), 1.43 (2H, m, H<sub>2</sub>-4), 1.42 (1H, m, H-8a), 1.28 (2H, m, H<sub>2</sub>-11), 1.27 (2H, m, H<sub>2</sub>-9), 1.27 (2H, m, H<sub>2</sub>-10), 1.13 (3H, d, *J* = 6.9 Hz, H<sub>3</sub>-13), 0.87 (3H, t, *J* = 7.0 Hz, H<sub>3</sub>-12); HRESIMS *m/z* 274.2386 [M+H]<sup>+</sup> (calcd for C<sub>15</sub>H<sub>32</sub>NO<sub>3</sub>, 274.2382)
15. (*S*)-MTPA ester of **2** (**2S**): Compound **2** (0.4 mg) was dissolved in 200 μL of dry CH<sub>2</sub>Cl<sub>2</sub>. Then, 5 μL of (*R*)-MTPA chloride and catalytic amount of DMAP were added into the solution. After standing overnight at room temperature, the reaction mixture was concentrated *in vacuo* and re-dissolved in MeOH. The product was purified by reversed phase ODS HPLC using a gradient from 75 to 95 % aqueous MeOH for 40 min to yield 0.3 mg of **2S**. (*S*)-MTPA ester (**2S**): colorless oil; <sup>1</sup>H NMR data (600 MHz, CDCl<sub>3</sub>) δ 7.48 – 7.56 (2H, m, Ar-H), 7.39 – 7.41 (3H, m, Ar-H), 5.31 (1H, m, NH), 5.30 (1H, m, H-5), 3.60 (3H, s, OCH<sub>3</sub>), 3.26 (3H, s, OCH<sub>3</sub>), 3.06 (1H, m, H-7), 2.74 (3H, d, *J* = 4.9 Hz, NCH<sub>3</sub>), 2.07 (1H, m, H-2), 1.73 (1H, ddd, *J* = 14.7, 9.3 and 2.8 Hz, H-6b), 1.58 (1H, m, H-6a), 1.53 (2H, m, H<sub>2</sub>-4), 1.52 (1H, m, H-3b), 1.49 (1H, m, H-8b), 1.35 (1H, m, H-8a), 1.28 (2H,

m, H<sub>2</sub>-11), 1.24(1H, m, H-3a), 1.24 (2H, m, H<sub>2</sub>-9), 1.24 (2H, m, H<sub>2</sub>-10), 1.03 (3H, d, *J* = 6.9 Hz, H<sub>3</sub>-13), 0.86 (3H, t, *J* = 7.3 Hz, H<sub>3</sub>-12); HRESIMS *m/z* 512.2592 [M+Na]<sup>+</sup> (calcd for C<sub>25</sub>H<sub>38</sub>NO<sub>5</sub>Na, 512.2600)

16. (*R*)-MTPA ester of **2** (**2R**): Compound **2R** was prepared from **2** and (*S*)-MTPA chloride in the same manner as described for **2S**. (*R*)-MTPA ester (**2R**): colorless oil; <sup>1</sup>H NMR data (600 MHz, CDCl<sub>3</sub>) δ 7.48 – 7.56 (2H, m, Ar-H), 7.39 – 7.41 (3H, m, Ar-H), 5.39 (1H, m, NH), 5.29 (1H, m, H-5), 3.60 (3H, s, OCH<sub>3</sub>), 3.23 (3H, s, OCH<sub>3</sub>), 2.93 (1H, m, H-7), 2.77 (3H, d, *J* = 4.9 Hz, NCH<sub>3</sub>), 2.13 (1H, m, H-2), 1.66 (1H, ddd, *J* = 14.6, 9.5 and 2.5 Hz, H-6b), 1.64 (1H, m, H-3b), 1.63 (2H, m, H<sub>2</sub>-4), 1.53 (1H, m, H-6a), 1.43 (1H, m, H-8b), 1.37 (1H, m, H-3a), 1.27 (1H, m, H-8a), 1.24 (2H, m, H<sub>2</sub>-11), 1.17 (2H, m, H<sub>2</sub>-9), 1.17 (2H, m, H<sub>2</sub>-10), 1.08 (3H, d, *J* = 6.9 Hz, H<sub>3</sub>-13), 0.85 (3H, t, *J* = 7.2 Hz, H<sub>3</sub>-12); HRESIMS *m/z* 512.2595 [M+Na]<sup>+</sup> (calcd for C<sub>25</sub>H<sub>38</sub>NO<sub>5</sub>Na, 512.2600)

17. Absolute configuration of the 2-hydroxyisovaleric acid residue (**3**): A portion of **1** (200 μg) was hydrolyzed in 6 N HCl (1 mL) at 110°C for 16 h. The acid hydrolysate of **1** was evaporated to dryness and then re-dissolved in 200 μL of water. HPLC analysis was carried out on a chiral column by comparing the retention times of the components of the hydrolysate with those of authentic standards. Condition: 15% CH<sub>3</sub>CN in 2 mM CuSO<sub>4</sub>, 1 ml/min, Phenomenex Chirex phase 3126 (4.6 × 250 mm) column; elution times (*t*<sub>R</sub>, min) for standards: *L*-2-hydroxyisovaleric acid (34.2 min), *D*-2-hydroxyisovaleric acid (53.3 min). The acid hydrolysate of **1** exhibited a peak at 34.3 min, corresponding to *L*-2-hydroxyisovaleric acid.

18. Jones, A. D.; Monroe, E. A.; Eisman, E. B.; Gerwick, L.; Sherman, D. H.; Gerwick, W. H. *Nat. Prod. Rep.* **2010**, 27, 1048-1065.